

(S)

EUROPEAN ORGANIZATION FOR NUCLEAR RESEARCH

CERN LIBRARIES, GENEVA

CERN-PPE/94-116

14 July 1994



CERN-PPE-94-116

SW 34 32

**SPIN ASYMMETRY IN MUON-PROTON DEEP INELASTIC
SCATTERING ON A TRANSVERSELY-POLARIZED TARGET**

The Spin Muon Collaboration (SMC)

Abstract

We measured the spin asymmetry in the scattering of 100 GeV longitudinally-polarized muons on transversely polarized protons. The asymmetry was found to be compatible with zero in the kinematic range $0.006 < x < 0.6$, $1 < Q^2 < 30 \text{ GeV}^2$. From this result we derive the upper limits for the virtual photon-proton asymmetry A_2 , and for the spin structure function g_2 . For $x < 0.15$, A_2 is significantly smaller than its positivity limit \sqrt{R} .

Submitted to Physics Letters B

D. Adams¹⁹, B. Adeva²¹, E. Arik², A. Arvidson²⁴, B. Badelek^{24,26}, M.K. Ballintijn¹⁶,
G. Bardin²⁰, G. Baum¹, P. Berglund⁹, L. Betev¹⁴, I.G. Bird^{20,a}, R. Birsa²³,
P. Björkholm²⁴, B.E. Bonner¹⁹, N. de Botton²⁰, F. Bradamante²³, A. Bressan²³,
A. Brüll^{7,c}, S. Bültmann¹, E. Burtin²⁰, C. Cavata²⁰, M. Clocchiatti²³, M.D. Corcoran¹⁹,
D. Crabb²⁵, J. Cranshaw¹⁹, M. Crawford⁴, T. Çuhadar², S. Dalla Torre²³,
R. van Dantzig¹⁶, S. Dhawan²⁷, C. Dulya³, A. Dyring²⁴, S. Eichblatt¹⁹, J.C. Faivre²⁰,
D. Fasching¹⁸, F. Feinstein²⁰, C. Fernandez^{21,10}, B. Frois^{5,20}, J.A. Garzon^{21,10},
T. Gaussiran¹⁹, M. Giorgi²³, E. von Goeler¹⁷, G. Gracia²¹, N. de Groot¹⁶, M. Grosse
Perdekamp³, E. Gülmez², D. von Harrach¹², T. Hasegawa^{15,c}, P. Hautle^{6,d},
N. Hayashi^{15,k}, C.A. Heusch⁴, N. Horikawa¹⁵, V.W. Hughes²⁷, G. Igo³, S. Ishimoto^{15,f},
T. Iwata¹⁵, E.M. Kabuß¹², R. Kaiser⁷, A. Karev¹¹, H.J. Kessler⁷, T.J. Ketel¹⁶,
A. Kishi¹⁵, Yu. Kisselev¹¹, L. Klostermann¹⁶, D. Krämer¹, V. Krivokhijine¹¹,
V. Kukhtin¹¹, J. Kynäräinen^{5,9}, M. Lamanna²³, U. Landgraf⁷, K. Lau¹⁰, T. Layda⁴,
J.M. Le Goff²⁰, F. Lehar²⁰, A. de Lesquen²⁰, J. Lichtenstadt²², T. Lindqvist²⁴,
M. Litmaath¹⁶, S. Lopez-Ponte^{21,10}, M. Lowe¹⁹, A. Magnon^{5,20}, G.K. Mallot^{12,5},
F. Marie²⁰, A. Martin²³, J. Martino²⁰, T. Matsuda^{15,e}, B. Mayes¹⁰, J.S. McCarthy²⁵,
K. Medved¹¹, G. van Middelkoop¹⁶, D. Miller¹⁸, K. Mori¹⁵, J. Moromisato¹⁷,
A. Nagaitsev¹¹, J. Nassalski²⁶, L. Naumann⁵, T.O. Niinikoski⁵, J.E.J. Oberski¹⁶,
D.P. Parks¹⁰, A. Penzo²³, C. Perez²¹, F. Perrot-Kunne²⁰, D. Peshekhonov¹¹,
R. Piegai^{5,27,g}, L. Pinsky¹⁰, S. Platchkov²⁰, M. Plo²¹, D. Pose¹¹, H. Postma¹⁶, J. Pretz¹²,
T. Pussieux²⁰, J. Pyrlik¹⁰, I. Reyhancan², J.M. Rieubland⁵, A. Rijllart⁵, J.B. Roberts¹⁹,
S. Rock^{5,i}, M. Rodriguez²¹, E. Rondio²⁶, A. Rosado¹⁴, I. Sabo²², J. Saborido²¹,
A. Sandacz²⁶, I. Savin¹¹, P. Schiavon²³, K.P. Schüller^{27,h}, R. Segel¹⁸, R. Seitz¹²,
Y. Semertzidis⁵, F. Sever^{16,j}, P. Shanahan¹⁸, N. Shumeiko⁴, G. Smirnov¹¹, A. Staude¹⁴,
A. Steinmetz¹², U. Stiegler⁵, H. Stuhmann⁸, K.M. Teichert¹⁴, F. Tessarotto²³,
M. Velasco¹⁸, J. Vogt¹⁴, R. Voss⁵, R. Weinstein¹⁰, C. Whitten³, R. Windmolders¹³,
R. Willumeit⁸, W. Wislicki²⁶, A. Witzmann⁷, A.M. Zanetti²³, J. Zhao⁸

-
- 1) University of Bielefeld, Physics Department, 33501 Bielefeld, Germany^m
 - 2) Boğaziçi University, Çekmece Nuclear Research Center, Istanbul Technical University, Istanbul University, Turkey^l
 - 3) University of California, Department of Physics, Los Angeles, 90024 CA, USAⁿ
 - 4) University of California, Institute of Particle Physics, Santa Cruz, 95064 CA, USA
 - 5) CERN, 1211 Geneva 23, Switzerland
 - 6) ETH, 8093 Zürich, Switzerland
 - 7) University of Freiburg, Physics Department, 79104 Freiburg, Germany^m
 - 8) GKSS, 21494 Geesthacht, Germany^m
 - 9) Helsinki University of Technology, Low Temperature Laboratory, Otakaari 3A, 02150 Finland
 - 10) University of Houston, Department of Physics, Houston, 77204-5504 TX, and Institute for Beam Particle Dynamics, Houston, 77204-5506 TX, USA^{n,o}
 - 11) JINR, Laboratory of Super High Energy Physics, Dubna, Russia
 - 12) University of Mainz, Institute for Nuclear Physics, 55099 Mainz, Germany^m
 - 13) University of Mons, Faculty of Science, 7000 Mons, Belgium
 - 14) University of Munich, Physics Department, 80799 Munich, Germany^m
 - 15) Nagoya University, Department of Physics, Furo-cho, Chikusa-Ku, 464 Nagoya, Japan^p
 - 16) NIKHEF, Delft University of Technology, FOM and Free University, 1009 AJ Amsterdam, The Netherlands^q
 - 17) Northeastern University, Department of Physics, Boston, 02115 MA, USA^o
 - 18) Northwestern University, Department of Physics, Evanston, 60208 IL, USA^{n,o}
 - 19) Rice University, Bonner Laboratory, Houston, 77251-1892 TX, USAⁿ
 - 20) DAPNIA, C.E. Saclay, 91191 Gif-sur-Yvette, France
 - 21) University of Santiago, Department of Particle Physics, 15706 Santiago de Compostela, Spain^r
 - 22) Tel Aviv University, School of Physics, 69978 Tel Aviv, Israel^s
 - 23) INFN Trieste and University of Trieste, Department of Physics, 34127 Trieste, Italy
 - 24) Uppsala University, Department of Radiation Sciences, 75121 Uppsala, Sweden
 - 25) University of Virginia, Department of Physics, Charlottesville, 22901 VA, USA^o
 - 26) Warsaw University and Soltan Institute for Nuclear Studies, 00681 Warsaw, Poland^t
 - 27) Yale University, Department of Physics, New Haven, 06511 CT, USAⁿ
 - a) Now at CERN, 1211 Geneva 23, Switzerland
 - b) Now at University of Montreal, PQ, H3C 3J7, Montreal, Canada
 - c) Now at Max Planck Institute, Heidelberg, Germany
 - d) Permanent address: Paul Scherrer Institut, 5232 Villigen, Switzerland
 - e) Permanent address: Miyazaki University, 88921 Miyazaki-Shi, Japan
 - f) Permanent address: KEK, 305 Ibaraki-Ken, Japan
 - g) Permanent address: University of Buenos Aires, Physics Department, 1428 Buenos Aires, Argentina
 - h) Now at SSC Laboratory, Dallas, 75237 TX, USA
 - i) Permanent address: The American University, Washington D.C. 20016, USA.
 - j) Present address: ESRF, F-38043 Grenoble, France.
 - k) Research Fellow of JSPS
 - l) Partially supported by TUBITAK and Centre for Turkish-Balkan Physics Research and Applications (Boğaziçi University)
 - m) Supported by Bundesministerium für Forschung und Technologie
 - n) Supported by the U.S. Department of Energy
 - o) Supported by the National Science Foundation

The nucleon spin-dependent structure functions, g_1 and g_2 , can be determined in deep inelastic scattering of polarized charged leptons on polarized nucleons. Both are important for the understanding of nucleon spin structure. The structure function g_1 is used to test QCD sum rules, and in the quark-parton model it determines the contribution of the quark spins to the nucleon spin. The spin structure function g_2 differs from zero because of the masses and the transverse momenta of the quarks. It has a unique leading-order sensitivity to twist-3 operators, i.e., quark-gluon correlation effects in QCD. The measurement of g_2 would provide the first information on these twist-3 operator matrix elements [1].

In general, g_2 can be written as the sum of a contribution, g_2^{ww} , directly calculable from g_1 [2], and a pure twist-3 term \overline{g}_2 [1]

$$g_2(x, Q^2) = g_2^{ww}(x, Q^2) + \overline{g}_2(x, Q^2), \quad (1)$$

with

$$g_2^{ww}(x, Q^2) = -g_1(x, Q^2) + \int_x^1 g_1(t, Q^2) \frac{dt}{t}, \quad (2)$$

where $-Q^2$ is the four-momentum transfer squared, and x is the Bjorken scaling variable. In several recent papers, values for \overline{g}_2 and their approximate Q^2 dependence have been calculated using different assumptions [3, 4, 5, 6]. A sum rule for g_2 ,

$$\int_0^1 g_2(x, Q^2) dx = 0, \quad (3)$$

was derived by Burkhardt and Cottingham using Regge theory [7]. It has been regarded as a consequence of conservation of angular momentum [8]. At present the validity of the derivation of this sum rule is in question [9, 1], and it is clearly important to test it experimentally.

Two kinds of spin-dependent cross-section asymmetries can be measured in inclusive lepton-nucleon scattering. When the target polarization is parallel to the direction of the longitudinally-polarized beam, the asymmetry is given by A_{\parallel} , whilst for a target polarized in a direction transverse to the beam, the asymmetry is given by A_T

$$A_{\parallel}(x, Q^2) = \frac{d\sigma^{11} - d\sigma^{\bar{1}\bar{1}}}{d\sigma^{11} + d\sigma^{\bar{1}\bar{1}}}, \quad A_T(x, Q^2, \phi) = \frac{d\sigma^{1-} - d\sigma^{\bar{1}-}}{d\sigma^{1-} + d\sigma^{\bar{1}-}}. \quad (4)$$

Here, $d\sigma^{11}(d\sigma^{\bar{1}\bar{1}})$ corresponds to $d^2\sigma/dx dQ^2$ for parallel (antiparallel) beam and target polarization. For perpendicular target polarisation, $d\sigma^{1-}(d\sigma^{\bar{1}-})$ stands for $d^3\sigma/dx dQ^2 d\phi$, when the target spin points in the upwards (downwards) direction. The azimuthal angle ϕ is defined about the beam axis, $\phi = 0$ corresponding to a muon scattered upwards. It can be shown that A_T is proportional to $\cos\phi$, and thus it is convenient to define $A_{\perp}(x, Q^2) \equiv A_T(x, Q^2, \phi)/\cos\phi$, which is independent of ϕ [1].

^{p)} Supported by Ishida Foundation, Mitsubishi Foundation and Monbusho International Science Research Program

^{q)} Supported by the National Science Foundation (NWO) of the Netherlands

^{r)} Supported by Comision Interministerial de Ciencia y Tecnologia

^{s)} Supported by the US-Israel Binational Science Foundation, Jerusalem, Israel and The Israeli Academy of Sciences

^{t)} Supported by KBN grant nr. 20958-9101

^{u)} Permanent address: Belarussian State University, Minsk, Belarus.

The virtual photon absorption asymmetries

$$A_1 = \frac{\sigma_{1/2} - \sigma_{3/2}}{\sigma_{1/2} + \sigma_{3/2}}, \quad A_2 = \frac{2\sigma_{TL}}{\sigma_{1/2} + \sigma_{3/2}}, \quad (5)$$

are related to the measured asymmetries A_{\parallel} and A_{\perp} ,

$$A_{\parallel} = D \left(A_1 + \gamma \frac{(1-y)}{1-y/2} A_2 \right) \quad (6)$$

$$A_{\perp} = d \left(A_2 - \gamma \left(1 - \frac{y}{2}\right) A_1 \right). \quad (7)$$

Here $\sigma_{1/2}$ and $\sigma_{3/2}$ are the virtual photon–nucleon absorption cross sections for total helicity 1/2 and 3/2, respectively, and σ_{TL} arises from the helicity spin-flip amplitude in forward photon–nucleon Compton scattering [10, 11]. The kinematic factor γ is defined by $\gamma = \sqrt{Q^2}/\nu = 2Mx/\sqrt{Q^2}$, where ν is the energy transfer in the laboratory frame, and $y = \nu/E_{\mu}$. The coefficient d is related to the virtual photon depolarization factor D by

$$d = D \frac{\sqrt{1-y}}{1-y/2} \quad D = \frac{y(2-y)}{y^2 + 2(1-y)(1+R)}. \quad (8)$$

where R is the ratio of the longitudinal to transverse photoabsorption cross sections, σ_L/σ_T . In the case of A_{\parallel} , the contribution of the A_2 term relative to A_1 is suppressed by a factor γ . The opposite is true for the case of A_{\perp} .

Positivity conditions [12] limit the magnitudes of A_1 and A_2

$$|A_1| < 1, \quad |A_2| \leq \sqrt{R}. \quad (9)$$

The asymmetries A_1 and A_2 can be expressed in terms of the structure functions g_1 and g_2

$$A_1 = \frac{1}{F_1}(g_1 - \gamma^2 g_2), \quad A_2 = \frac{\gamma}{F_1}(g_1 + g_2). \quad (10)$$

where $F_1 = F_2(1 + \gamma^2)/2x(1 + R)$ is the spin-independent structure function. The ratio R , determined at SLAC [13], is about 0.3 in the range $0.1 < x < 0.4$ for $Q^2 \cong 1.5 \text{ GeV}^2$, and similar values are usually assumed at smaller x . Using these values of R , the positivity condition on A_2 [Eq. (9)] combined with Eq. (10) leads to an upper limit for $|g_2|$ which is approximately of the form $|x^2 g_2| < K$, where K varies from 0.07 to 0.10. Thus, large values of g_2 are allowed in the low x region.

In the past, only A_{\parallel} has been measured in polarized deep inelastic experiments on the proton. The asymmetry A_1 has been extracted from these measurements by neglecting the contribution of the A_2 term. In this paper we present data on A_{\perp} , which makes it possible to extract A_1 and A_2 with no approximations [Eqs. (6) and (7)]. The A_1 results have been published in Ref. [14]. In this Letter, we present the results for the asymmetry A_2 , and for the structure function g_2 .

The experiment was carried out at the CERN SPS by scattering 100 GeV longitudinally-polarized muons off transversely-polarized protons. The polarized target and the spectrometer used for these measurements are basically the same as those used to measure longitudinal asymmetries, and have been described in a previous publication [14]. The new SMC target incorporates a sufficiently strong dipole field of 0.5 T [15], in which the

proton polarization can be maintained transverse to the beam direction. The two cells of the butanol target, each 60 cm long, were longitudinally polarized along a solenoid field of 2.5 T by dynamic nuclear polarization (DNP). When high polarization was reached, the proton spins were ‘frozen’ at a base temperature of about 60 mK, and rotated to a transverse (vertical) direction by applying the additional dipole field and reducing the longitudinal field to zero. Upwards (downwards) transverse polarization was achieved by choosing the initial longitudinal polarization parallel (antiparallel) to the beam direction. The spins were reversed 10 times during the 17 days of data-taking. The transverse field was always applied in the same direction to avoid different acceptances. As it was not possible to measure the polarization in the transverse spin direction at 0.5 T, it was measured before and after each reversal in the solenoid field at 2.5 T. The loss of polarization was less than 1 % over a period of 12 h. The average polarization was $P_T = 0.80 \pm 0.04$.

The deflection of the incoming muons caused by the transverse dipole field was 2.25 mrad, and was compensated by an additional magnet, installed 7 m upstream of the target. The reconstruction software was modified to account for the curvature of the beam tracks in the region between the two sets of scintillator hodoscopes used to determine their direction. Track reconstruction and vertex fitting inside the dipole field were tested by a Monte Carlo simulation, and were found to perform just as well as in the case of the solenoid field used for longitudinal asymmetry measurements.

The incident muons mostly come from pion decay and are naturally polarized in the longitudinal direction. The average beam polarization at 100 GeV was determined from the positron energy spectrum in the decay $\mu^+ \rightarrow e^+ \nu_e \bar{\nu}_\mu$, and found to be $P_B = -0.82 \pm 0.06$ [16, 17], in good agreement with the Monte Carlo simulation of the beam transport [18].

The events were required to satisfy $y < 0.9$, $E_{\mu'} > 15$ GeV, and $\nu > 10$ GeV, in order to avoid large radiative corrections, to eliminate muons originating from the decay of pions produced in the target, and events with poor kinematic resolution. A total of 8.7×10^5 events was obtained in the range $0.006 < x < 0.6$ and $1 < Q^2 < 30$ GeV². The event distribution as a function of the angle ϕ is shown in Fig. 1. Most events are collected in the regions where the angle ϕ is close to zero or π because the trigger conditions predominantly select muons scattered in a direction close to the vertical plane. This optimizes our measurement, because only muons scattered in a plane close to the polarization plane contribute effectively to the asymmetry.

The asymmetries were obtained separately for each target cell. The raw asymmetry A_m is measured in bins of x , Q^2 , and ϕ from the number of scattered muons (N_1, N_2) in the azimuthal directions ($\phi, \pi - \phi$), and the corresponding counts (N'_1, N'_2) evaluated after a reversal of the polarization. Assuming that the ratio of the spectrometer acceptances at angles ϕ and $\pi - \phi$ is the same during the periods before and after polarization reversal, we obtain

$$\sqrt{\frac{N_1 N'_2}{N_2 N'_1}} = \frac{1 + A_m(x, Q^2, \phi)}{1 - A_m(x, Q^2, \phi)} \quad (11)$$

The transverse asymmetry is then

$$A_\perp(x, Q^2) = \frac{1}{\cos \phi} \frac{A_m(x, Q^2, \phi)}{P_B |P_T| f}, \quad (12)$$

where P_B and P_T are the beam and target polarizations, and f is the fraction of polarizable protons in the target material ($f \cong 0.12$). The values of A_\perp corresponding to the same x

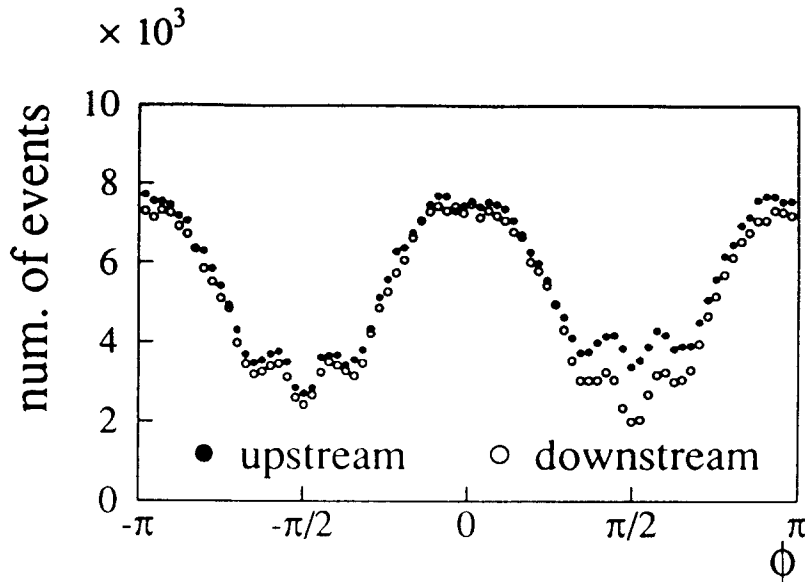


Figure 1: The event distribution as a function of the azimuthal angle ϕ , for interactions in the upstream and downstream targets. The value $\phi = 0$ corresponds to a scattered muon with transverse momentum parallel to the target polarization. The observed distribution mainly reflects the trigger acceptance.

and Q^2 are averaged over the ϕ intervals, and over the five subsamples defined by the ten polarization reversals.

The asymmetry A_2 is extracted from A_{\perp} and A_{\parallel} in (x, Q^2) bins, using Eqs. (6) and (7). For A_{\parallel} we use previous measurements on longitudinally polarized targets [19, 20, 14]. These experiments have published A_1 , extracted through the relation $A_1 = A_{\parallel}/D$, where the A_2 contribution is neglected. We parametrize the A_1 data and recover A_{\parallel} through the same relation.

Since no Q^2 dependence is observed within the errors, we present the average of A_2 in each bin of x (see Table 1). If the \bar{g}_2 contribution can be neglected in Eq. (1) and A_1 is independent of Q^2 , $\sqrt{Q^2}A_2$ is expected to scale. However, if we average $\sqrt{Q^2}A_2$, instead of A_2 , we obtain the same results.

The dominant systematic error on A_{\perp} is the variation of the ratio of acceptances in the upper and lower parts of the spectrometer between polarization reversals. The resulting false asymmetries have been studied using real data and a Monte Carlo simulation, and found to be negligible compared to the statistical error. Radial effects and overall variations in detector efficiencies do not cause false asymmetries because they affect the upper and lower part of the spectrometer in the same way. The radiative corrections to A_{\perp} were calculated with the method of Ref. [21] and found to be smaller than 0.001.

The resulting values for A_{\perp} are shown in Fig. 2, for four intervals of x . They are consistent for the two parts of the target and are compatible with zero.

The corresponding values of A_2 are presented in Fig. 3 and Table 1. The limit imposed by the positivity condition (Eq. 9) is also shown in Fig. 3. The present measurements constrain the asymmetry function A_2 to values much smaller than the positivity limit. At 90 % confidence level, we obtain $A_2 < 0.16$ for $x < 0.15$, and $A_2 < 0.4$ for $x > 0.15$. These improved limits have been used in Ref. [14] for the evaluation of g_1 . The expected values of A_2 obtained by considering only the first term of g_2 in Eq. 1 are also

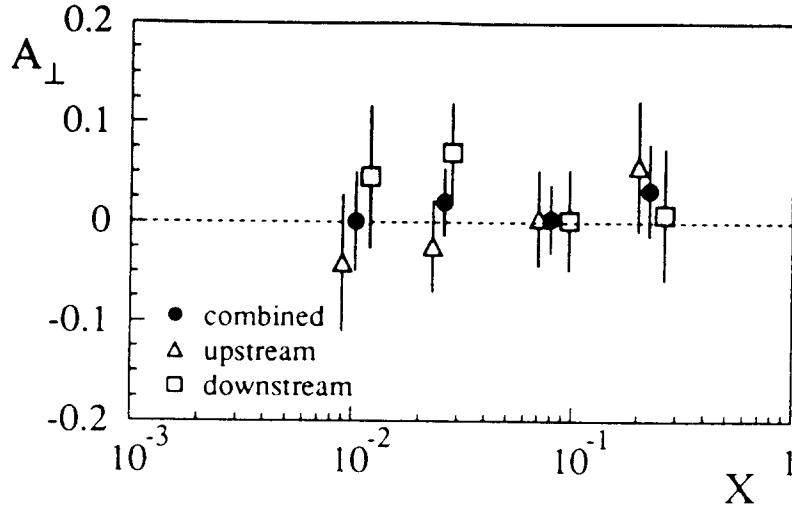


Figure 2: The transverse cross-section asymmetry A_{\perp} as a function of x for interactions in the upstream and downstream targets and for the combined data. The error bars represent the statistical errors.

shown in Fig. 3, and are in good agreement with the data. They have been calculated from the values of g_1 from Refs. [19, 20, 14] assuming that g_1 scales with F_1 . Additional sources of systematic errors in A_2 are the parametrization of longitudinal asymmetries, and the uncertainty in R . Both effects are smaller than 10 % of the statistical error.

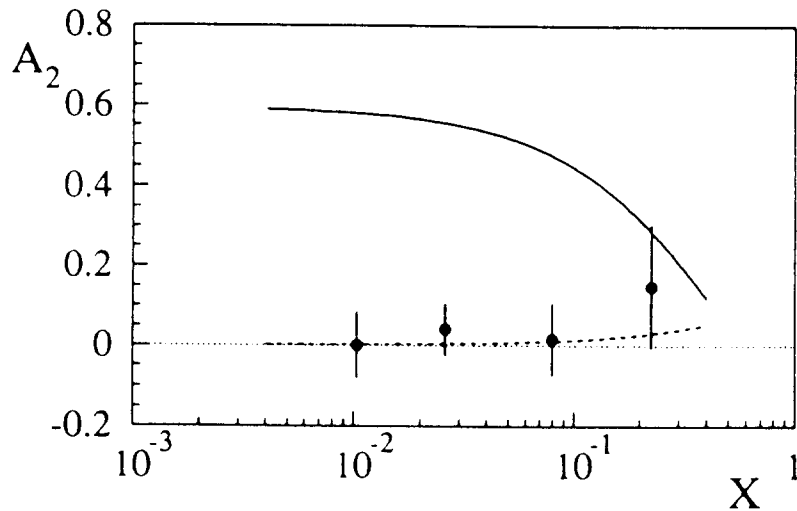


Figure 3: The asymmetry A_2 as a function of x . The solid line shows \sqrt{R} from the SLAC parametrization [12], and the dashed line the results obtained with $\bar{g}_2 = 0$ in Eq. (1). The error bars represent statistical errors, only.

The values obtained for g_2 are listed in Table 1, together with those of g_2^{**} (Eq. 2) evaluated at the same x and Q^2 . The two sets are compatible within the statistical errors.

Table 1: Results on the spin asymmetry A_2 and the structure functions g_2 and g_2^{ww} , where g_2^{ww} has been calculated from the results of Ref. [19, 20, 14]. Only the statistical errors are given.

x interval	$\langle x \rangle$	$\langle Q^2(\text{GeV}^2) \rangle$	A_2	g_2	g_2^{ww}
0.006 – 0.015	0.010	1.4	0.002 ± 0.083	1.2 ± 61	0.73 ± 0.10
0.015 – 0.050	0.026	2.7	0.041 ± 0.066	7.0 ± 12	0.47 ± 0.09
0.050 – 0.150	0.080	5.8	0.017 ± 0.091	0.2 ± 2.9	0.15 ± 0.02
0.150 – 0.600	0.226	11.8	0.149 ± 0.156	0.5 ± 0.8	-0.10 ± 0.02

Therefore the present data do not show evidence for \bar{g}_2 to be different from zero. The limited accuracy of the present data does not allow sensitive tests of specific predictions, such as the partial cancellation between the two terms of g_2 predicted by the bag models of Refs. [3, 6]. Large contributions of \bar{g}_2 close to the positivity limit are excluded in the x range covered. However, \bar{g}_2 about one order of magnitude larger than g_2^{ww} would still be allowed within the statistical errors.

When the minimum Q^2 requirement is reduced to 0.5 GeV^2 , the data with $Q^2 < 1 \text{ GeV}^2$ in the lowest x -bin yield $A_2 = 0.05 \pm 0.10$, which is consistent with the value for $Q^2 > 1 \text{ GeV}^2$. If we neglect the Q^2 dependence within the kinematic range of the present data, the results of Table 1 can be used to calculate the limits for the integral of g_2 ,

$$-0.9 < \int_{0.006}^{0.6} g_2 dx < 1.9, \quad (13)$$

at 90 % confidence level. We do not attempt the evaluation of the first moment of g_2 , in order to test the Burkhardt–Cottingham sum rule, because we are not aware of theoretical predictions for the behaviour of g_2 as $x \rightarrow 0$.

In summary, we have presented the first measurement of transverse asymmetries in deep inelastic lepton–proton scattering. The virtual-photon asymmetry A_2 is found to be significantly smaller than its positivity limit \sqrt{R} . This result reduces the uncertainty in the determination of the structure function g_1 from longitudinal polarization measurements. In addition, bounds are obtained for the spin-dependent structure function g_2 , which exclude large twist-3 contributions.

References

- [1] R.L. Jaffe, *Comments Nucl. Part. Phys.* **19** (1990) 239.
- [2] S. Wandzura and F. Wilczek, *Phys. Lett.* **B72** (1977) 195.
- [3] M. Stratmann, *Z. Phys.* **C60** (1993) 763.
- [4] C. Chou and X. Ji, *Phys. Rev.* **D42** (1990) 3637.
- [5] A. Ali, V.M. Braun and G. Hiller, *Phys. Lett.* **B266** (1991) 117.
- [6] R.L. Jaffe and X. Ji, *Phys. Rev.* **D43** (1991) 724.
- [7] H. Burkhardt and W.N. Cottingham, *Ann. Phys.* **56** (1970) 453.
- [8] R.P. Feynman, in 'Photon-Hadron Interactions', Benjamin, 1972.
- [9] L. Mankiewicz and A. Schäfer, *Phys. Lett.* **B265** (1991) 167.
- [10] B.L. Ioffe, V.A. Khoze, L.N. Lipatov, in 'Hard Processes', North-Holland, Amsterdam, 1984, p. 59.
- [11] F.E. Close, in 'An Introduction to Quarks and Partons', Academic Press, New York, 1979, p. 296.
- [12] M.G. Doncel and E. de Rafael, *Nuovo Cimento* **4A** (1971) 363.
- [13] L.W. Whitlow et al., *Phys. Lett.* **B250** (1990) 193.
- [14] SMC, D. Adams et al., *Phys. Lett.* **B329** (1994) 399.
- [15] A. Daël, and D. Cacaut et al., *IEEE Trans. Magn.*, No. 1, **28** (1992).
- [16] SMC, B. Adeva et al., *Phys. Lett.* **B302** (1993) 533.
- [17] SMC, B. Adeva et al., *Nucl. Instrum. Methods* **A343** (1994) 363.
- [18] N. Doble, L. Gatignon et al., *Nucl. Instrum. Methods* **A343** (1994) 351.
- [19] M.J. Alguard et al., SLAC E-80, *Phys. Rev. Lett.* **37** (1976) 1261;
ibid. **41** (1978) 70; G. Baum et al., SLAC E-130, *Phys. Rev. Lett.* **51** (1983) 1135.
- [20] EMC, J. Ashman et al., *Phys. Lett.* **B206** (1988) 364; *Nucl. Phys.* **B328** (1989) 1.
- [21] T.V. Kukhto and N.M. Shumeiko, *Nucl. Phys.* **B219** (1983) 412;
I.V. Akushevich and N.M. Shumeiko, *J. Phys.* **G20** (1994) 513.